

Structural transition of LiBeH₃ under high pressure

Çağatay YAMÇICIER¹, Selgin AL^{2*}

¹ Department of Electric and Energy, Osmaniye Korkut Ata University, Osmaniye, Türkiye.

² Department of Environmental Protection Technologies, Izmir Democracy University, Izmir, Türkiye.

Received: 18 October 2022; Revised: 8 November 2022; Accepted: 18 November 2022

*Corresponding author e-mail: selgin.al@idu.edu.tr

Citation: Yamçicier, Ç.; Al, S. *Int. J. Chem. Technol.* 2022, 6 (2), 129-134.

ABSTRACT

LiBeH₃ has been considered as a solid-state hydrogen storage material. This study investigated Pnma orthorhombic phase of LiBeH₃ under pressure. Ab initio constant pressure molecular dynamic simulation under pressure was adopted. The results depicted a phase transition from Pnma orthorhombic phase to P2₁/m monoclinic phase at 270 GPa simulation pressure. The stability of each phase was examined using elastic constants. Based on the well-known Born stability criteria, both phases showed mechanical stability. Several moduli have been computed via elastic constants. The B/G ratios, Cauchy pressures and Poisson's ratios investigation revealed that LiBeH₃ is brittle at Pnma phase whereas it is ductile at P2₁/m phase. The electronic band structures and partial and total density of states of phases were also obtained. A 2.058 eV band gap was seen for Pnma phase, and 3 eV band gap was seen for P2₁/m phase.

Keywords: Phase transition, ab initio, elastic properties, stability.

Yüksek basınç altında LiBeH₃'ün yapısal faz geçişinin incelenmesi

ÖZ

LiBeH₃, katı hal hidrojen depolama malzemesi olarak literatürde çalışılmaktadır. Bu çalışma, basınç altında LiBeH₃'ün Pnma ortorombik fazını araştırmaktadır. Ab initio sabit basınç moleküler dinamik simülasyonu kullanılmıştır. Sonuçlar, 270 GPa simülasyon basıncında Pnma ortorombik fazdan P2₁/m monoklinik faza bir faz geçişini göstermektedir. Her fazın kararlılığı, elastik sabitler kullanılarak incelenmiştir. Born stabilite kriterlerine göre, her iki faz da mekanik kararlılık göstermektedir. Elastik sabitler aracılığıyla diğer modüller de hesaplanmıştır. B/G oranları, Cauchy basınçları ve Poisson oranları, LiBeH₃'ün Pnma fazında kırılma yapıya sahip olduğunu, P2₁/m fazında ise sünek yapıya sahip olduğunu göstermektedir. Elektronik bant yapıları incelendiğinde, Pnma fazı için 2.058 eV bant aralığı, P2₁/m fazı için 3 eV bant aralığı görülmektedir.

Anahtar Kelimeler: Faz geçişi, ab initio, elastik özellikler, kararlılık.

1. INTRODUCTION

The continues increase in world population and fast urbanization has caused a dramatic rise in energy consumption and demand. Most of this demand is still met by using hydrocarbon fuels and classic ways of producing electricity which has resulted in an increase in CO₂ emissions and other greenhouse gases. This created climate change crises and global warming. One of the popular options to mitigate climate change is that adopting renewable energy which provides a shift from hydrocarbon-based energy production to clean and

sustainable energy production. One challenge with that approach is to store energy to avoid fluctuations and setbacks. Recently, hydrogen has been suggested as a reliable energy carrier to ease the problem of storing and transporting renewable energy safely.^{1,2} Hence, there is growing research in literature to shift carbon-free energy generation using hydrogen as a carrier. Hydrogen energy requires four main stages: production, storage, transport, and end use. There are several materials under investigation for each stage. Hydrogen can be stored in different ways, compressed hydrogen storage, liquid hydrogen, metal hydrides and chemical hydrides.³ The elemental metal hydrides such as magnesium hydride

(MgH₂) and aluminum hydride (AlH₃) has been studied extensively.⁴⁻⁶ Due to slow kinetics of hydrogenation and dehydrogenation and strong bond between magnesium and hydrogen MgH₂ is still under investigation. Light metal hydrides are under intense investigation due to their high hydrogen gravimetric density. LiBeH₃ is one of the studied materials which exists in different symmetries. The experimental studies are very little since Be is very toxic and requires precautions. Thus, most properties of LiBeH₃ were investigated computationally. The elastic properties of cubic and orthorhombic LiBeH₃ was studied by Rehmat et al.⁷ It was reported that LiBeH₃ can be used as active photocatalyst for green hydrogen production.⁸ The electronic and mechanical properties of cubic and orthorhombic LiBeH₃ have been studied theoretically.⁹⁻¹¹ In this study, elastic and electronic properties of orthorhombic LiBeH₃ will be studied by adopting first principles calculations. Also, phase transitions of LiBeH₃ will be examined under high pressure. The obtained phases then will be evaluated for phase stability.

2. METHOD OF COMPUTATION

The ab initio computations were adopted within the density functional theory as implemented in SIESTA method in order to calculate structural, elastic, and electronic properties of LiBeH₃.¹² Perdew-Burke-Ernzerhof, generalised gradient approximation (PBE-GGA) was used for the exchange correlation potential.¹³ A 8x8x8 k-points mesh was taken to sample the Brillouin zone. The electronic wave functions were expanded in plane-wave basis to set up a kinetic energy cut off to 30 Ry, while the cut off energy for the electronic charge density was set to 300 Ry. LiBeH₃ was modelled using 2x2x2 cells with periodic boundary conditions for 160 atoms supercells. The Brillouin zones (BZ) were sampled with the 8x6x8 and 8x8x8 Monkhorst-Pack k-point mesh for Pnma and P2₁/m structures, respectively.

3. RESULTS AND DISCUSSION

3.1 Structural evolution

Firstly, the formation energy of LiBeH₃ has been computed as -0.221 eV. The negative formation energy indicates synthesizability and dynamic stability. Then pressure was applied to the structure. The volume change under pressure using the simulation cell (160 atoms with a 2x2x2 cells) is shown in Figure 1. V/V_0 represents a reduction in volume compared to zero pressure volume. The cell parameters at 0 GPa (Pnma phase) are $a = 4.6167$ Å, $b = 6.4320$ Å and $c = 4.5438$ Å. The volume of simulation cell drops at 270 GPa about 3.90 %, and a phase transition from Pnma to P2₁/m is observed. The cell parameters are 4.5217 Å, $b = 4.5762$ Å and $c = 4.7251$ Å. The atomic structures at both phases are illustrated in Figure 2.

It is possible to estimate the transition pressure higher than the actual phase transition due to adopting perfect structures and boundary conditions during the simulation¹⁴⁻¹⁸ Hence, the thermodynamic theorem to calculate the transition pressure was also used. The energy-volume calculations have been carried out and presented in Figure 2 and Figure 4. The details of calculation was given in ref.¹⁹ It can be seen from Figure 4 that both phases cross each other at 34 GPa, suggesting that the transition from Pnma phase to P2₁/m phase occurs at 34 GPa.

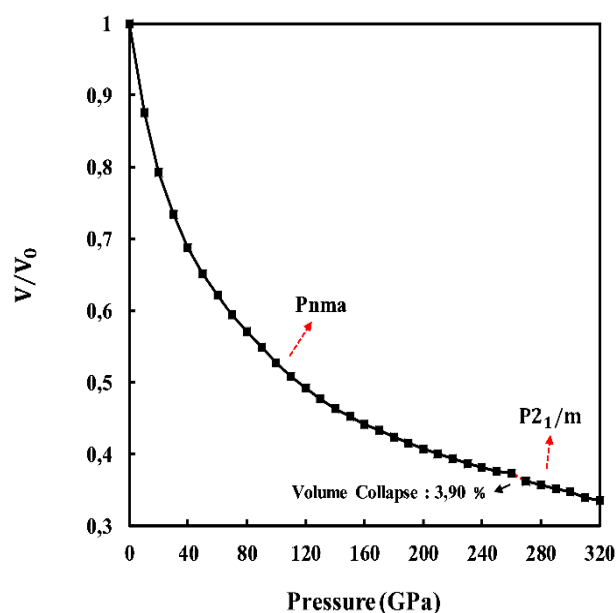


Figure 1. The change in volume of LiBeH₃ under hydrostatic pressure.

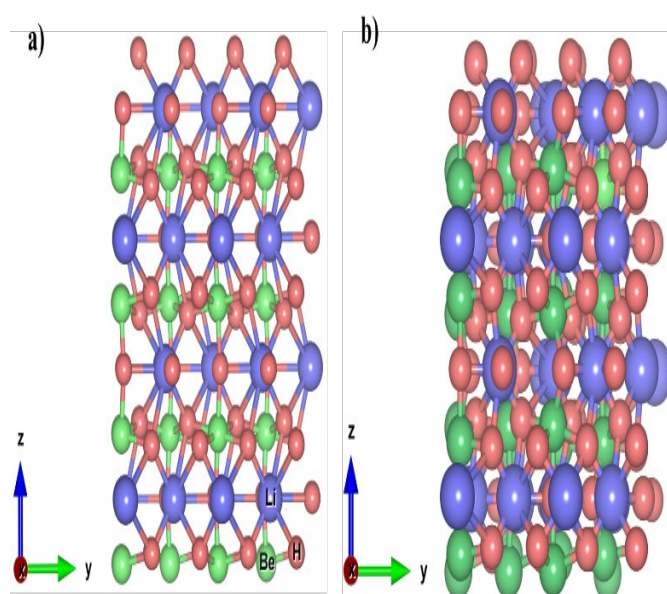


Figure 2. The structure of LiBeH₃ at a) 0 GPa (Pnma) b) 270 GPa (P2₁/m).

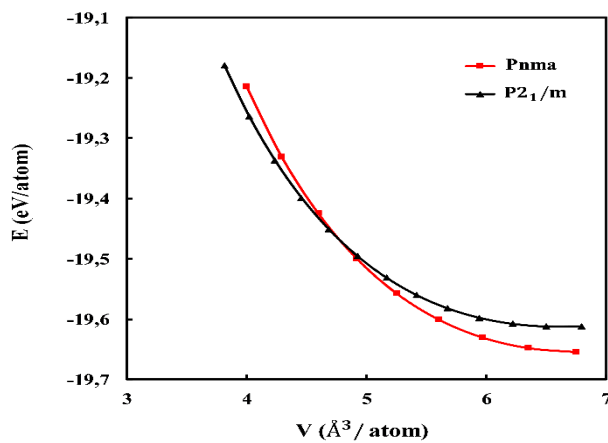


Figure 3. Energy volume of LiBeH₃ phases.

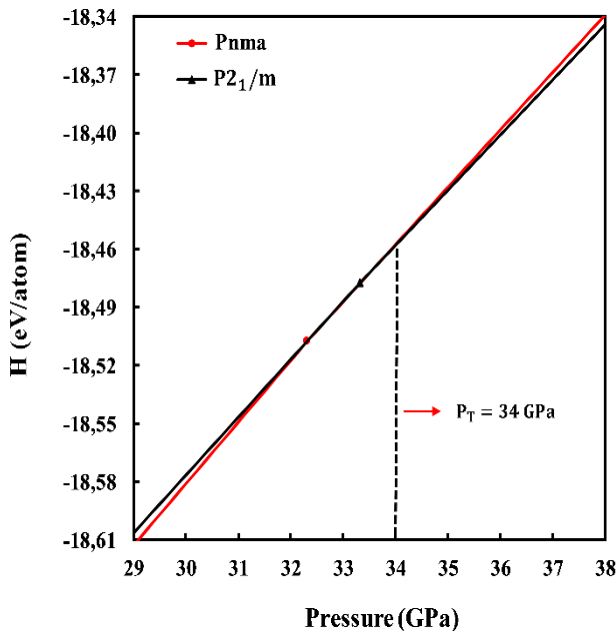


Figure 4. Enthalpy changes of phases under pressure.

3.2 Elastic properties

Table 1. The obtained elastic constants (GPa) of phases of LiBeH₃.

Phases	C ₁₁	C ₁₂	C ₁₃	C ₁₅	C ₂₂	C ₂₃	C ₂₅	C ₃₃	C ₃₅	C ₄₄	C ₄₆	C ₅₅	C ₆₆	Refs.
<i>Pnma</i>	96.41	38.13	32.41	-	100.05	27.73	-	93.78	-	52.34	-	36.46	60.65	This study
<i>P2₁/m</i>	685.49	252.96	414.79	58.11	757.95	297.67	-4.72	680.11	-83.74	238.18	-8.01	113.94	217.97	This study

Table 2. The calculated Bulk modulus (*B*, GPa), Shear modulus *G* (GPa), Young's modulus *E* (GPa), *B/G* and *G/B* ratios, and Poisson's ratios (σ) of phases of LiBeH₃.

Phases	<i>B</i>	<i>G</i>	<i>E</i>	<i>B/G</i>	<i>G/B</i>	σ	Refs.
<i>Pnma</i>	54.00	41.17	98.49	1.31	0.76	0.196	This study
<i>P2₁/m</i>	449.75	162.65	435.47	2.77	0.36	0.339	This study

Elastic constants of materials provide information about materials' response when an external pressure is applied along with mechanical properties.^{20,21} For an orthorhombic structure, there are nine elastic constants defined as C_{11} , C_{22} , C_{33} , C_{44} , C_{55} , C_{66} , C_{12} , C_{13} , C_{23} .^{22,23} The well-known Born criteria for an orthorhombic structure is given as;^{24,25}

$$\begin{aligned}
 &C_{11} + C_{33} - 2C_{13} > 0, \quad C_{22} + C_{33} - 2C_{23} > 0, \quad C_{11} + C_{22} - 2C_{12} > 0, \\
 &C_{11} > 0, \quad C_{22} > 0, \quad C_{33} > 0, \quad C_{44} > 0, \quad C_{55} > 0, \quad C_{66} > 0, \\
 &C_{11} + C_{22} + C_{33} + 2(C_{12} + C_{13} + C_{23}) > 0, \\
 &1/3 (C_{12} + C_{13} + C_{23}) < B < (C_{11} + C_{22} + C_{33}) \quad (1)
 \end{aligned}$$

There are thirteen independent elastic constants are defined for a low symmetry monoclinic structure as C_{ij} .^{26,27} Born stability criteria is defined as;^{28,29}

$$\begin{aligned}
 &C_{33}C_{55} - C_{35}^2 > 0, \quad C_{44}C_{66} - C_{46}^2 > 0, \\
 &C_{22} + C_{33} - 2C_{23} > 0 \quad C_{11} + C_{22} + C_{33} + 2(C_{12} + C_{13} + C_{23}) > 0 \\
 &C_{22}(C_{33}C_{55} - C_{35}^2) + 2C_{23}C_{25}C_{35} - C_{23}^2C_{55} - C_{25}^2C_{33} > 0, \\
 &2[C_{15}C_{25}(C_{33}C_{12} - C_{13}C_{23}) + C_{15}C_{35}(C_{22}C_{13} - C_{12}C_{23}) + C_{25}C_{35}(C_{11}C_{23} - C_{12}C_{13})] - [C_{15}^2(C_{22}C_{33} - C_{23}^2) + C_{25}^2(C_{11}C_{33} - C_{13}^2) + C_{35}^2(C_{11}C_{22} - C_{12}^2)] + gC_{55} > 0, \\
 &\text{With } g = C_{11}C_{22}C_{33} - C_{11}C_{23}^2 - C_{22}C_{13}^2 - C_{33}C_{12}^2 + 2C_{12}C_{13}C_{23} \quad (2)
 \end{aligned}$$

As can be seen from Table 1 that both *Pnma* and *P2₁/m* phase is mechanically stable. In order to investigate mechanical properties of phases, other crucial parameters have been calculated using elastic constants and presented in Table 2. Bulk modulus of LiBeH₃ was found to be 54 GPa in this study which is in a good agreement with ref.¹¹ (59.82 GPa) and ref.⁷ (68.17 GPa). There is no data found in literature to compare bulk modulus of *P2₁/m* phase of LiBeH₃.

Brittleness and ductility of LiBeH_3 was examined using B/G, G/B and Cauchy pressures. It was stated that a B/G ratio higher than 1.75 indicates ductility and a B/G ratio lower than 1.75 indicates brittleness.^{30,31} In addition, Pettifor³² stated that Cauchy pressure can also provide information about ductility/brittleness and bonding characteristics. Negative Cauchy pressure implies brittleness and directional angular or covalent bonding whereas positive Cauchy pressure indicates ductility and predominance of ionic bonding characteristics. For an orthorhombic structure, Cauchy pressure is $C_{23}-C_{44}$ for (100) plane, $C_{13}-C_{55}$ for (010) plane and $C_{12}-C_{66}$ for (001) plane.³³ Pnma phase of LiBeH_3 has a B/G ratio of 1.31 which lower than 1.75, thus Pnma phase of LiBeH_3 is brittle. Cauchy pressures are -24.61 for (100) plane, -4.05 for (010) plane and -22.52 for (001) plane. The negative values of Cauchy pressures also suggest brittleness and angular/covalent nature. On the other hand, $P2_1/m$ phase of LiBeH_3 shows ductile nature since its B/G ratio is higher than 1.75. Cauchy pressures for $P2_1/m$ phase is calculated similar to Pnma phase.³⁴ It is found as 59.49 GPa for (100) plane, 300.85 GPa for (010) plane and 34.99 GPa for (001) plane. The positive values of Cauchy pressure confirm ductile nature of $P2_1/m$ phase of LiBeH_3 .

Frantsevich et al.³⁵ also stated that Poisson's ratio (σ) can be used to determine ductility and brittleness of materials by the ratio of 0.26. If the Poisson's ratio is less than 0.26, the material is brittle, if it is higher than 0.26, it is classified as ductile. By evaluating, Poisson's ratios of phases, it can be confirmed that Pnma phase of LiBeH_3 is brittle and $P2_1/m$ phase of LiBeH_3 is ductile. Shear modulus (G) of materials describe materials response against shape change. Young modulus (E) gives information about stiffness. By comparing two phases, it is seen that $P2_1/m$ phase will show higher resistance towards shape change and stiffer compared to Pnma phase.

In addition to polycrystal elastic constants, Vickers hardness and melting point of LiBeH_3 is also computed. Vickers hardness is obtained from $H_V^G = 0.1769G - 2.899$ and $H_V^E = 0.0608E$ relation and melting point is computed using $T_m = 354 + 4.5(2C_{11} + C_{33})/3$ relation.^{36,37} From our calculations, $H_V^G = 4.38$ GPa and $H_V^E = 5.98$ GPa are obtained for Pnma phase. Both values are less than 10 GPa, thus Pnma phase of LiBeH_3 cannot be classified as a hard material. The melting point of Pnma phase of LiBeH_3 is obtained as 783.9 K. For $P2_1/m$ phase of LiBeH_3 , $H_V^G = 25.87$ GPa and $H_V^E = 26.47$ GPa are obtained. It is seen that $P2_1/m$ phase of LiBeH_3 is a hard material. The melting point is computed as 3430 K for $P2_1/m$ phase.

3.3 Electronic properties

In order to investigate electronic properties of phases, the electronic band structures and partial and total density of states have been computed and presented in Figure 5 and

Figure 6 for both phases. 0 eV was determined as Fermi energy level. As can be seen from Figures that band gaps are present for both phases. Pnma phase has 2.058 eV band gap whereas $P2_1/m$ phase has 3 eV band gap. The band gap seems to increase with pressure. H-1s states seem to contribute to the valence band for both phases. Be-2s states seem to contribute to the conduction band along with H-1s states.

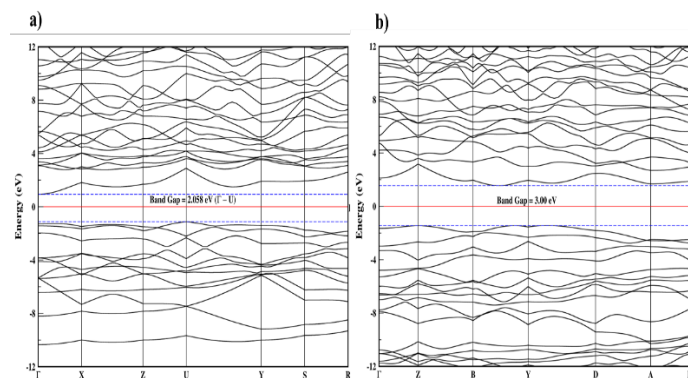


Figure 5. The calculated electronic band structures of LiBeH_3 at 0 GPa and at 270 GPa.

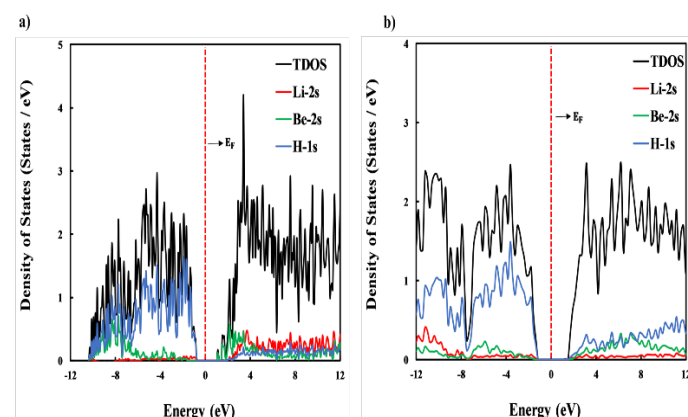


Figure 6. The partial and total DOS of LiBeH_3 at 0 GPa and at 270 GPa

4. CONCLUSION

This study investigated the structural, mechanical and electronic properties of LiBeH_3 under pressure. A phase transition from Pnma phase to $P2_1/m$ phase was observed at 34 GPa. The elastic constants evaluation depicted that both phases are mechanically stable. The B/G ratio, Cauchy pressure and Poisson's ratio of Pnma phase implied that Pnma phase of LiBeH_3 is brittle which might require extra attention when handling it. On the other hand, $P2_1/m$ phase was found to be ductile. The electronic band structure of phases showed band gap, indicating that both phases of LiBeH_3 is insulating.

Conflict of interests

I declares that there is no a conflict of interest with any institute, person, company, etc.

References

1. Ajanovic, A.; Sayer, M.; Haas, R., The economics and the environmental benignity of different colors of hydrogen. *Int. J. Hydrogen Energy* **2022**, *47* (57), 24136-24154.
2. Dawood, F.; Anda, M.; Shafiullah, G. M., Hydrogen production for energy: An overview. *Int. J. Hydrogen Energy* **2020**, *45* (7), 3847-3869.
3. Andersson, J.; Grönkvist, S., Large-scale storage of hydrogen. *Int. J. Hydrogen Energy* **2019**, *44* (23), 11901-11919.
4. Wolverton, C.; Ozoliņš, V.; Asta, M., Hydrogen in aluminum: First-principles calculations of structure and thermodynamics. *PhRvB* **2004**, *69* (14), 144109.
5. Züttel, A., Materials for hydrogen storage. *Mater. Today* **2003**, *6* (9), 24-33.
6. Andreasen, A., Hydrogenation properties of Mg–Al alloys. *Int. J. Hydrogen Energy* **2008**, *33* (24), 7489-7497.
7. Rehmat, B.; Rafiq, M. A.; Javed, Y.; Irshad, Z.; Ahmed, N.; Mirza, S. M., Elastic properties of perovskite-type hydrides LiBeH₃ and NaBeH₃ for hydrogen storage. *Int. J. Hydrogen Energy* **2017**, *42* (15), 10038-10046.
8. Reshak, A. H., Photocatalytic water splitting solar-to-hydrogen energy conversion: Perovskite-type hydride XBeH₃ (X=Li or Na) as active photocatalysts. *J. Catal.* **2017**, *351*, 119-129.
9. Xiao-Jiao, S.; Zhi, H.; Yan-Ming, M.; Tian, C.; Bing-Bing, L.; Guang-Tian, Z., Electronic structure and optical properties of LiXH₃ and XLiH₃ (X= Be, B or C). *Chinese Physics B* **2008**, *17* (6), 2222-2228.
10. Santhosh, M.; Rajeswarapalanichamy, R.; Priyanga, G. S.; Kanagaprabha, S.; Murugan, A.; Iyakutti, K., A first principles study of structural stability, electronic structure and mechanical properties of ABeH₃ (A = Li, Na). **2015**, *1665* (1), 090015.
11. Vajeeston, P.; Ravindran, P.; Fjellvåg, H., Structural Phase Stability Studies on MBeH₃ (M = Li, Na, K, Rb, Cs) from Density Functional Calculations. *Inorg. Chem.* **2008**, *47* (2), 508-514.
12. Ordejón, P.; Artacho, E.; Soler, J. M., Self-consistent order-N density-functional calculations for very large systems. *PhRvB* **1996**, *53* (16), R10441.
13. Perdew, J. P.; Burke, K.; Ernzerhof, M., Generalized Gradient Approximation Made Simple. *Phys. Rev. Lett.* **1996**, *77* (18), 3865-3868.
14. Yamçicier, C.; Merdan, Z.; Kurkcu, C., Investigation of the structural and electronic properties of CdS under high pressure: an ab initio study. *Can. J. Phys.* **2017**, *96* (2), 216-224.
15. Kürkçü, C.; Selgin, A.; Merdan, Z.; Yamçicier, Ç.; Öztürk, H., Investigation of structural and electronic properties of β-HgS: Molecular dynamics simulations. *ChJPh* **2018**, *56* (3), 783-792.
16. Durandurdu, M., Orthorhombic intermediate phases for the wurtzite-to-rocksalt phase transformation of CdSe: An ab initio constant pressure study. *Chem. Phys.* **2010**, *369* (2-3), 55-58.
17. Kürkçü, C.; Merdan, Z.; Öztürk, H., Theoretical calculations of high-pressure phases of NiF₂: An ab initio constant-pressure study. *Russian Journal of Physical Chemistry A* **2016**, *90* (13), 2550-2555.
18. Kürkçü, C.; Merdan, Z.; Öztürk, H., Pressure-induced phase transitions and structural properties of CoF₂: An ab-initio molecular dynamics study. *Solid State Communications* **2016**, *231*, 17-25.
19. Al, S.; Kurkcu, C.; Yamçicier, C., Structural evolution, mechanical, electronic and vibrational properties of high capacity hydrogen storage TiH₄. *Int. J. Hydrogen Energy* **2020**, *45* (55), 30783-30791.
20. Bougherara, K.; Litimein, F.; Khenata, R.; Uçgun, E.; Ocak, H.; Uğur, Ş.; Uğur, G.; Reshak, A. H.; Soyalt, F.; Omran, S. B., Structural, elastic, electronic and optical properties of Cu₃TMSe₄ (TM= V, Nb and Ta) sulvanite compounds via first-principles calculations. *J Science of Advanced Materials* **2013**, *5* (1), 97-106.
21. Benzoudji, F.; Abid, O. M.; Seddik, T.; Yakoubi, A.; Khenata, R.; Meradji, H.; Uğur, G.; Uğur, S.; Ocak, H. Y., Insight into the structural, elastic, electronic, thermoelectric, thermodynamic and optical properties of MRhSb (M= Ti, Zr, Hf) half-Heuslers from ab initio calculations. *J Chinese Journal of Physics* **2019**, *59*, 434-448.
22. Li, P.; Zhang, J.; Ma, S.; Zhang, Y.; Jin, H.; Mao, S., First-principles investigations on structural stability, elastic and electronic properties of Co₇M₆ (M= W, Mo, Nb) μ phases. *MoSim* **2019**, *45* (9), 752-758.
23. Subhan, F.; Azam, S.; Khan, G.; Irfan, M.; Muhammad, S.; Al-Sehemi, A. G.; Naqib, S. H.; Khenata, R.; Khan, S.; Kityk, I. V.; Amin, B., Elastic and optoelectronic properties of CaTa₂O₆ compounds:

Cubic and orthorhombic phases. *J. Alloys Compd.* **2019**, 785, 232-239.

24. Ali, I. O. A.; Joubert, D. P.; Suleiman, M. S. H., A theoretical investigation of structural, mechanical, electronic and thermoelectric properties of orthorhombic $\text{CH}_3\text{NH}_3\text{PbI}_3$. *The European Physical Journal B* **2018**, 91 (10), 263.
25. Rahmani, R.; Amrani, B.; Driss Khodja, K.; Boukhachem, A.; Aubert, P., Systematic study of elastic, electronic, and magnetic properties of lanthanum cobaltite oxide. *Journal of Computational Electronics* **2018**, 17 (3), 920-925.
26. Liu, Q.-J.; Liu, F.-S.; Liu, Z.-T., Structural, Mechanical, and Electronic Properties of Monoclinic $\text{N}_2\text{H}_5\text{N}_3$ Under Pressure. *BrJPh* **2015**, 45 (4), 399-403.
27. Edrees, S. J.; Shukur, M. M.; Obeid, M. M., First-principle analysis of the structural, mechanical, optical and electronic properties of wollastonite monoclinic polymorph. *Computational Condensed Matter* **2018**, 14, 20-26.
28. Weck, P. F.; Kim, E.; Buck, E. C., On the mechanical stability of uranyl peroxide hydrates: implications for nuclear fuel degradation. *RSC Advances* **2015**, 5 (96), 79090-79097.
29. Nan-Xi, M.; Chun-Ying, P.; Chao-Zheng, H.; Fei-Wu, Z.; Cheng, L.; Zhi-Wen, L.; Da-Wei, Z., Mechanical and thermodynamic properties of the monoclinic and orthorhombic phases of SiC_2N_4 under high pressure from first principles. *Chinese Physics B* **2014**, 23 (12), 127101.
30. Arıkan, N.; Örnek, O.; Charifi, Z.; Baaziz, H.; Uğur, Ş.; Uğur, G., A first-principle study of Os-based compounds: Electronic structure and vibrational properties. *J Journal of Physics Chemistry of Solids* **2016**, 96, 121-127.
31. Al, S., Investigations of Physical Properties of XTiH_3 and Implications for Solid State Hydrogen Storage. In *Zeitschrift für Naturforschung A*, 2019; Vol. 74, p 1023.
32. Pettifor, D., Theoretical predictions of structure and related properties of intermetallics. *J Materials Science and Technology* **1992**, 8 (4), 345-349.
33. Liu, L.; Wu, X.; Wang, R.; Nie, X.; He, Y.; Zou, X., First-principles investigations on structural and elastic properties of orthorhombic TiAl under pressure. *Crystals* **2017**, 7 (4), 111.
34. Ran, Z.; Zou, C.; Wei, Z.; Wang, H., VELAS: An open-source toolbox for visualization and analysis of elastic anisotropy. *Comput. Phys. Commun.* **2022**, 108540.
35. I.N. Frantsevich, F. F. V., S.A. Bokuta, *Elastic constants and elastic moduli of metals and insulators*. Naukova Dumka: Kiev, 1983.
36. Wang, S.-L.; Pan, Y., Insight into the structures, melting points, and mechanical properties of NbSi_2 from first-principles calculations. **2019**, 102 (8), 4822-4834.
37. Chen, H.; Yang, L.; Long, J., First-principles investigation of the elastic, Vickers hardness and thermodynamic properties of Al-Cu intermetallic compounds. *Superlattices Microstruct.* **2015**, 79, 156-165.